

Lateral accretion of modern unvegetated rivers: remotely sensed fluvial–aeolian morphodynamics and perspectives on the Precambrian rock record

ALESSANDRO IELPI*

Department of Earth Sciences, Laurentian University, Sudbury, ON, P3E 2C6, Canada

(Received 28 July 2015; accepted 10 March 2016; first published online 12 May 2016)

Abstract – Modern unvegetated rivers flowing through aeolian-dune fields demonstrate potential as analogues for pre-vegetation fluvial landscapes. A prominent example is contained in the Lençóis Maranhenses of Brazil, a coastal aeolian system hosting the semi-perennial Rio Negro. Remotely sensed images covering *c.* 45 years display the rhythmic expansion and wind-driven shift of single-threaded and sinuous fluvial trunks alternating with wider braided plains. Sinuous tracts feature mid-channel and bank-attached bars, including expansional point bars with subdued relief. The morphology, accretion and sediment transport of unvegetated point bars in the Rio Negro are compared to the morphodynamics of vegetated meandering rivers. Unvegetated point bars are composed of large coalescent unit bars, lack apparent scroll topography and are preferentially attached to channel banks located on the windward side of the river course. Unvegetated meanders have expansional behaviour related to downwind channel trailing. Point bars maintain an expansional planform despite spatial confinement induced by aeolian dunes. Channel-flow impingement onto cohesion-less banks favours scouring of deep pools along the bar tails, which host bank-collapse deposits subsequently reworked into new bars. Analogies to Precambrian rivers suggest that ancient unvegetated fluvial landscapes were not unequivocally featured by low sinuosity, especially if characterized by a low gradient and stable discharge. This inference is supported by ongoing studies on Proterozoic fluvial–aeolian systems in the Canadian Shield. Lack of scroll topography introduces overlap with low-sinuosity fluvial facies models, underscoring the value of observing ancient fluvial deposits in planform, or along 3D sections where the palaeodrainage of channel bodies and attached bars can be compared.

Keywords: meander, point bar, Proterozoic, pre-vegetation, desert, remote sensing, Brazil.

1. Introduction

The study of fluvial deposits pre-dating the expansion of land plants is highly topical in sedimentology for extra-terrestrial analogue modelling (Fairén *et al.* 2014) and mineral exploration (Jefferson *et al.* 2007). Pre-vegetation rivers have so far been considered largely non-actualistic (Eriksson *et al.* 2006) and, despite partial modern analogues proposed in some instances (Davies & Gibling, 2010), fully comparative systems are yet to be documented. Since the formulation of the sheet-braided model of Cotter (1978), pre-Silurian rivers are thought to have been dominated by large, shallow channels that readily shifted across alluvial plains with width:depth ratios possibly exceeding 1500 (Fuller, 1985; Rainbird, 1992). This model is demonstrated to be representative of Cambrian–Ordovician units (Davies & Gibling, 2010), but not of scattered Precambrian units (Long, 2011). The dominance of braided over meandering planforms in unvegetated settings has been questioned in some instances. For example, ancient unvegetated meandering-fluvial planforms are well preserved in extra-terrestrial realms with hydrologic cycles (Wood, 2006), whereas unequivocal

documentation of pre-Silurian fluvial planforms has been, so far, exceedingly rare (Buck, 1983; Ielpi & Rainbird, 2015). Some authors pointed out that the gradation between intermediate fluvial planforms is overlooked in the rock record (cf. Thomas *et al.* 2006), or that sheet-braided deposits may in fact comprise several fluvial styles (Santos *et al.* 2014).

Insight into this debate may be aided by multi-temporal analysis of modern fluvial–aeolian systems that lack vegetation and are largely composed of cohesion-less deposits. Fluvial–aeolian systems are in fact prominent yet underexplored depositional landscapes (Langford, 1989; Williams, 2015; Liu & Coulthard, 2015), and several well-exposed Precambrian examples have been documented (Pulvertaft, 1985; Tirsgaard & Øxnevad, 1998; Hadlari, Rainbird & Donaldson, 2006; Ielpi & Rainbird, 2015). This research explores the morphodynamics of unvegetated fluvial reaches of a sub-humid, coastal aeolian system, the Lençóis Maranhenses (Brazil), using a database of satellite scenes that covers a time span of *c.* 45 years. Multi-temporal analysis reveals that the Lençóis Maranhenses are transected by a semi-perennial fluvial trunk, the Rio Negro, which variously interconnects ponded interdunes. During peaks of fluvial activity, channels varying in morphology from single-threaded

*E-mail: aielpi@laurentian.ca

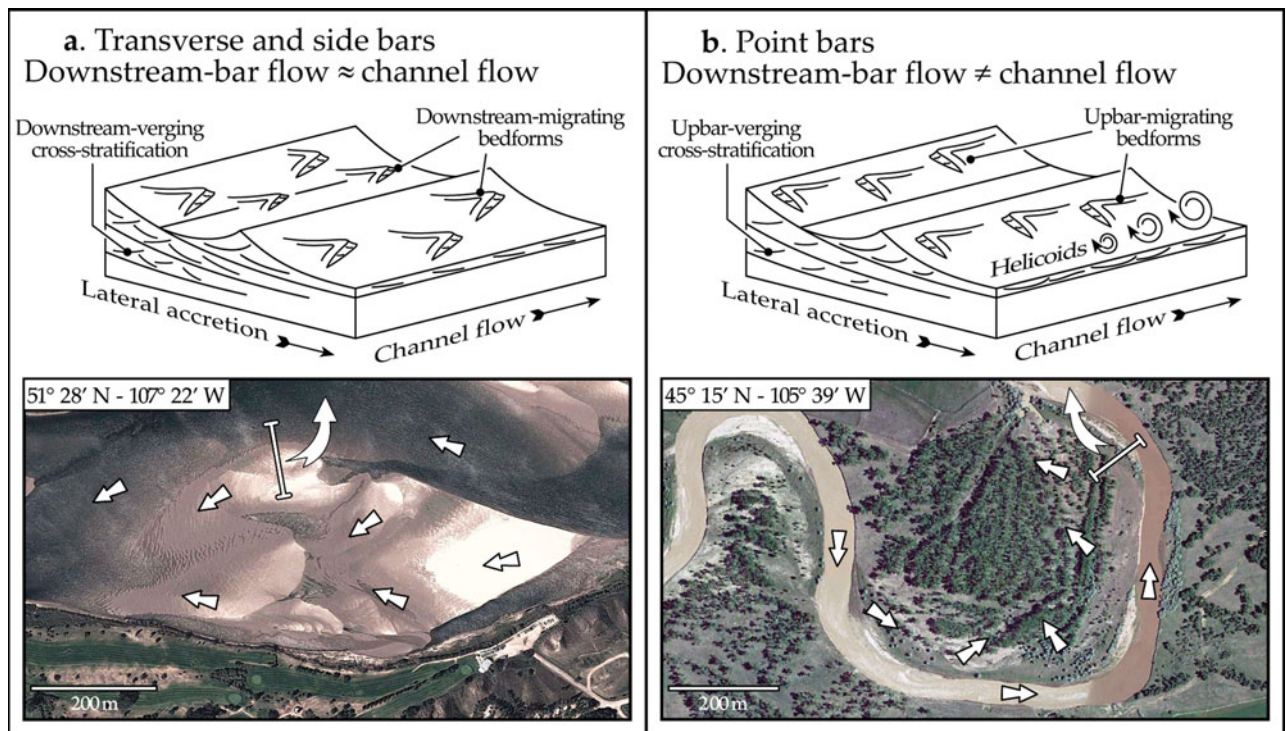


Figure 1. (Colour online) Block diagrams illustrating modern examples of fluvial lateral accretion. (a) Transverse and side bars exhibit downstream-bedform migration in a direction consistent with the channel flow (Cant & Walker, 1978a; Rust, 1981). (b) Point bars exhibit up-bar-bedform migration along their central and downstream portions (Allen, 1982), in a direction not consistent with that of the parent channel. White arrows indicate local flow; no scale is intended in the block diagrams. Note that bars with intermediate behaviour between (a) and (b) are a common feature of weakly sinuous rivers.

to braided exhibit a variety of fluvial forms, including point bars. The aims of this work are: (i) to document for the first time unvegetated, cohesion-less point bars through multi-temporal analysis of remote sensing supports; (ii) to characterize their morphodynamics through a comparison with vegetated meandering rivers; and (iii) to discuss these results in terms of Precambrian fluvial models. The outcomes of this work are purposely based on the remote sensing of modern environments yet, in their broader perspective, aim to stimulate a larger debate on the sedimentary record of unvegetated rivers draining sand-dominated, cohesion-less alluvial plains.

1.a. State of the art

Fluvial lateral accretion refers to growth of channel bars in a direction near-perpendicular to the channel axis. In braided rivers characterized by multiple, low-sinuosity channels, lateral accretion is often mixed with, and subordinate to, components of downstream accretion, which together bring about the configuration of mid-channel and bank-attached bars typically termed transverse bars and side bars, respectively (Cant & Walker, 1978a; Rust, 1981). In moderately to highly sinuous, single-thread channels, the configuration of stable and more prominent bank-attached bars (point bars) is more favourable, and these are often capable of incorporating smaller mid-channel bars during their outbuilding (Hooke, 1986).

Lateral accretion occurs with different modes, depending on the morphology and sinuosity of the channel itself. In straight to low-sinuosity channels, transverse and side bars are generated by the build-up of downstream-migrating bedforms; this process is related to significant bar mobility (cf. ‘free bars’ of Tubino, Repetto & Zolezzi, 1999). Transverse and side bars display sediment transport in a direction largely consistent with that of the parent channel (Bridge, 1993; Bartholdy & Billi, 2002; Fig. 1a). In high-sinuosity streams, bank-attached bars maintain a more stable position, and evolve through systematic outer-bank erosion and inner-bank deposition (cf. ‘fixed bars’ model of Seminara, 2006). Distortion of channel flow along sinuous bends promotes across-channel gradients in velocity, and development of helicoidal currents that induce sediment transport from the thalweg towards the bar top (‘point bars’ of Jackson, 1976; Allen, 1982). This process gains strength from central-to-downstream-bar portions, generating bedforms that migrate up-bar in bankward to upstream-oblique directions (Fig. 1b).

As the sedimentary product of ancient fluvial bars cannot be identified based on their original ‘free’ v. ‘fixed’ behaviour, the recognition of point bars in the rock record relies on the relationships between channel and bar flow, specifically of sediment-transport indicators pointing to up-bar bedform migration in a direction not consistent with that of the parent channel (Ielpi & Ghinassi, 2014). The recognition of ancient point

bars in many Siluro-Devonian and younger units has been used as circumstantial evidence that vegetation led to enhanced bank strengthening and bar stabilization (Davies & Gibling, 2010). By comparison, lateral accretion in pre-vegetation fluvial deposits has so far been identified in the form of side bars (Ethridge, Tyler & Burns, 1984; Todd & Went, 1991; Rainbird, 1992), while the unequivocal documentation of point bars remains very limited (Long, 2011; Ielpi & Rainbird, 2015; Santos & Owen, 2016).

2. Criteria and methods of analysis

A number of studies on modern rivers have postulated that vegetation has a dominant role in restraining wandering (thus favouring increase in sinuosity) in smaller channels, but a negligible effect where plant axes are more than 10^3 times smaller than the channel width (extrapolated from Zimmerman, Goodlett & Comer, 1967; Andrews, 1984; Church, 2002; Eaton & Giles, 2009). In support of this inference, flume experiments showed that vegetation coverage below 5% is unable to significantly influence fluvial planform (Gran & Paola, 2001; Tal & Paola, 2007). In this work, tracts of fluvial landscapes are defined as *unvegetated* where these criteria are met with a confidence of one order of magnitude, i.e. where plant coverage is less than 0.5%, and where the ratio between the diameter of vascular plant-axis (if any) and bankfull-channel width is 10^{-4} or less.

The database of this study includes a multi-temporal collection of satellite images and aerial photographs of unvegetated fluvial–aeolian and vegetated fluvial landscapes. The database consists of images acquired through vintage aerial photography and Landsat™ (pixel size = 15–60 m; retrieved from the US Geological Survey Earth Explorer), RapidEye™ (pixel size = 5 m; retrieved from Google™ Earth), and IKONOS™ and Quickbird™ (pixel size = 0.6–0.8 m; retrieved from Google™ Earth and Bing™ Maps). Long-term changes (i.e. at the decadal scale) in depositional planform are evaluated through direct comparison of overlapped, low-resolution images (aerial photographs and Landsat™). Short-term depositional morphodynamics (i.e. at the scale of months to a few years) are instead evaluated from satellite images with < 5 m of ground resolution, with flow indicators and direction of bar accretion collected taking into account the vector of progradation and sloping of bedforms, respectively.

3. The Lençóis Maranhenses

The Lençóis Maranhenses (Maranhão, Brazil) are a warm tropical, sub-humid aeolian-dune field facing the Southern Atlantic coast (Fig. 2a), with drainage controlled by external fluvial input into the aeolian-dune field, spatial confinement induced by aeolian-dune forms, and interdune connectivity mediated by aeolian-dune migration, level of the groundwater table and loss of channel discharge due to infiltration (Al-Masrahy &

Mountney, 2015). The aeolian field is largely composed of barcanoid dunes and trailing ridges, and developed in response to Quaternary widening of the Atlantic coastal shelf, followed by fast shoreline transgression and subsequent depositional regression, with abundant sand supply from local rivers (Miranda, Costa & Rocha, 2012). The mean annual temperature is 28.5 °C with less than 2 °C of variation throughout the year. The Rio Grande, Rio Sucuruíú and Rio Negro (RG, RS and RN in Figs 2b, 3) are the main fluvial trunks feeding into the aeolian-dune field. No major spring lines are observed, and the Rio Negro is the only river transecting the entire aeolian-dune field. The Rio Negro is named after the abundant dark-coloured tannins dissolved in its waters, a condition that makes the observation of in-channel planforms particularly favourable (Fig. 4b–e). Significant changes occurred in the planform of its tributary trunks and anabranches over the last 45 years (Fig. 2c). However, the final tract of the Rio Negro (the one seen in between the two large oases Queimada dos Britos and Baixa Grande; QB and BG in Fig. 2b) remained somewhat stable (Fig. 3), and represents the study area of this research.

Metre-scale fluctuations of the groundwater table are also controlled by precipitation, which varies from 1600 to 2400 mm year⁻¹. Rainfall related to the Inter-tropical Convergence Zone occurs from January to June and accounts for 70% of the annual precipitation (Castro & Piorski, 2002), whereas July to December are arid months. At highest groundwater-table level, roughly 40% of the dune field is flooded (Levin *et al.* 2006): most freshwater ponds are less than 1 m deep, and fluvial channels are 2 to 5 m deep. While scattered vegetation, consisting of *Cassia*, *Borreria* and Poaceae, stabilizes some protected environments within the dune field (Luna *et al.* 2011; Fig. 2), vast portions of the Lençóis Maranhenses lack any stabilizing vegetation (Hilbert, Guedes & Giannini, 2016), and the lower Rio Negro *de facto* meets the criteria for being considered unvegetated (Fig. 4). Since the availability of sediment in the study transect is strongly controlled by aeolian processes, the lower Rio Negro is devoid of fine-grained materials, and its channel banks are carved into sand-dominated, cohesion-less deposits.

3.a. Fluvial morphodynamics

Figures 2c and 3 report multi-temporal image sets of the Rio Negro, displaying active discharge and fluvial reworking of aeolian sand over a timespan of *c.* 45 years, with bankfull discharge during June–July, and limited embanked drainage during September–October. Aeolian dunes, ponded interdunes and fluvial tracts oriented parallel to the aeolian-dune crests underwent westward migration at a rate of *c.* 25 m year⁻¹ (Fig. 3a). Fluvial tracts draining in a direction oblique to near-opposite to that of the aeolian-dune crests had instead lower mobility, being subject to westward migration of less than 10 m year⁻¹ (Fig. 3b). In the stable tracts, nucleation and reworking of bank-attached bars

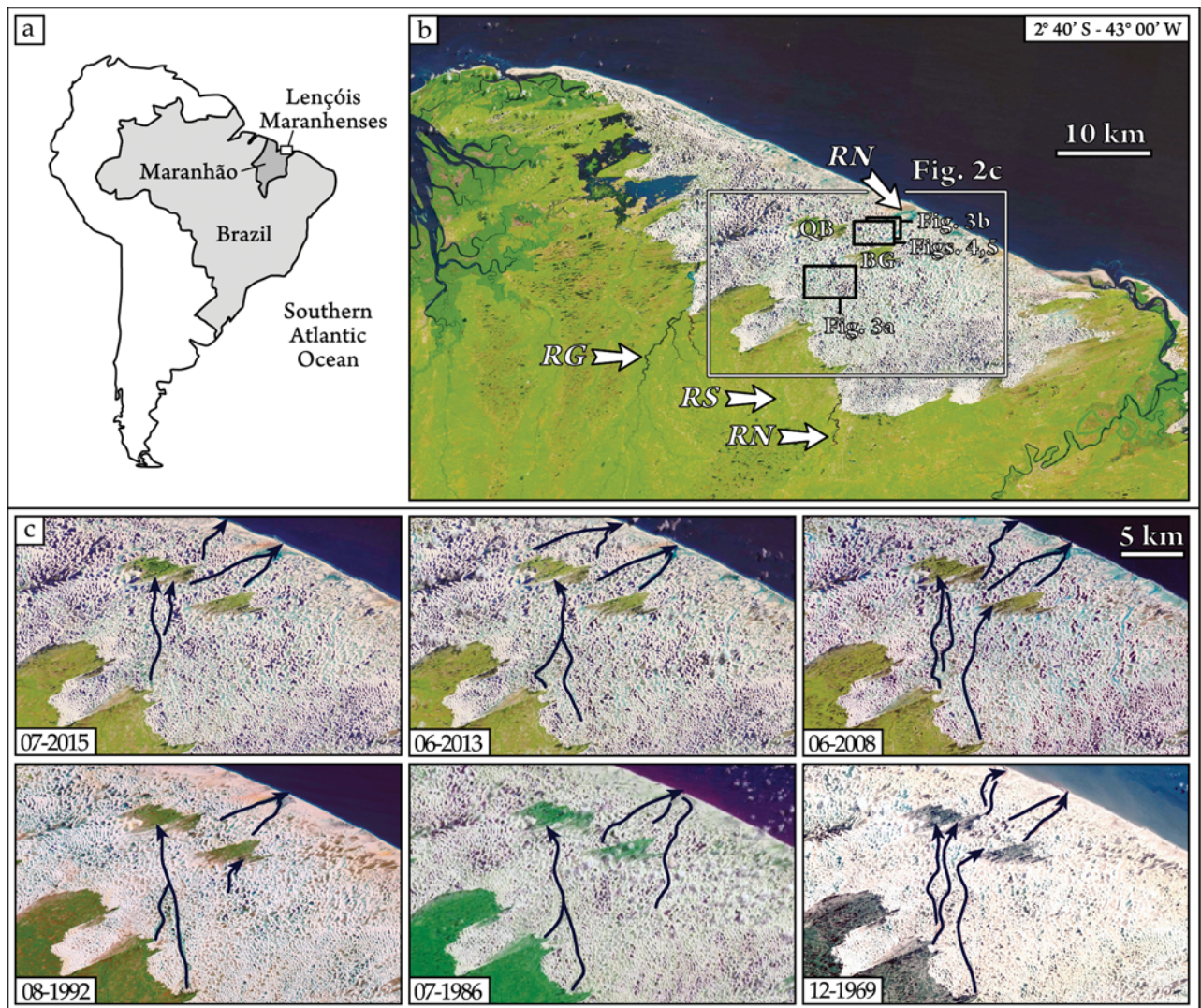


Figure 2. (Colour online) Geographic and geomorphologic setting. (a) Geographic sketch showing the location of the study area. (b) Regional Landsat™ view of the Lençóis Maranhenses, displaying the location of the insets in the following figures. White arrows point to active fluvial trunks feeding the aeolian-dune field. Abbreviations: RG – Rio Grande; RS – Rio Sucuruú; RN – Rio Negro; QB – Queimada dos Britos; BG – Baixa Grande. (c) Multi-temporal Landsat™ set of low-resolution, false-colour views of the Rio Negro and tributaries, over a timespan of *c.* 45 years (green patches represent areas of stable vegetation within, and at the border of, the aeolian-dune field). Major fluvial trunks are reported with blue arrowed lines.

takes place (Fig. 4a). Two individual sand-bed fluvial trunks joining in the vicinity of their outlet into the Atlantic Ocean are here detailed (Figs 4, 5). These fluvial trunks expanded and contracted repeatedly, spanning in width from a few tens of metres to some 700 m. Their width to depth ratios range from 40 to 350, values typical of broad, shallow sheet channels (cf. Gibling, 2006). The upstream reaches of the study river transect are both braided and single-threaded, the latter slightly sinuous (sinuosity index = 1.3). Sinuous trunks consist in some instances of channel anabranches lateral to the larger braided-channel belt. The downstream part of the transect consists instead of a wider, shallower and virtually straight channel belt. Planform sinuosity is controlled by adjacent aeolian dunes providing spatial confinement. Bank-attached bars develop in the upstream reaches along sharp channel bends (Fig. 4c, d).

In places, channel-flow impingement on the outer bank is inferred to be prominent enough to develop helicoidal currents (Figs 4c, 5). Outer-bank erosion takes place in concert with deposition along the inner bank, processes that bring about the development of fixed sediment bodies, i.e. point bars. Larger, isolated point bars show modest change during most of the channel-belt lifespan (e.g. December 1969 and October 2013 scenes in Fig. 4), while smaller point bars appear more unstable and tend to cluster together (Fig. 5). Downstream, the channel belt widens, and coalescent transverse bars are dominant (Fig. 4e). During periods of very low flow activity (October 2013 scene in Fig. 4a), upstream reaches are readily buried under migrating aeolian dunes, while downstream reaches undergo entrenching as the groundwater level lowers.

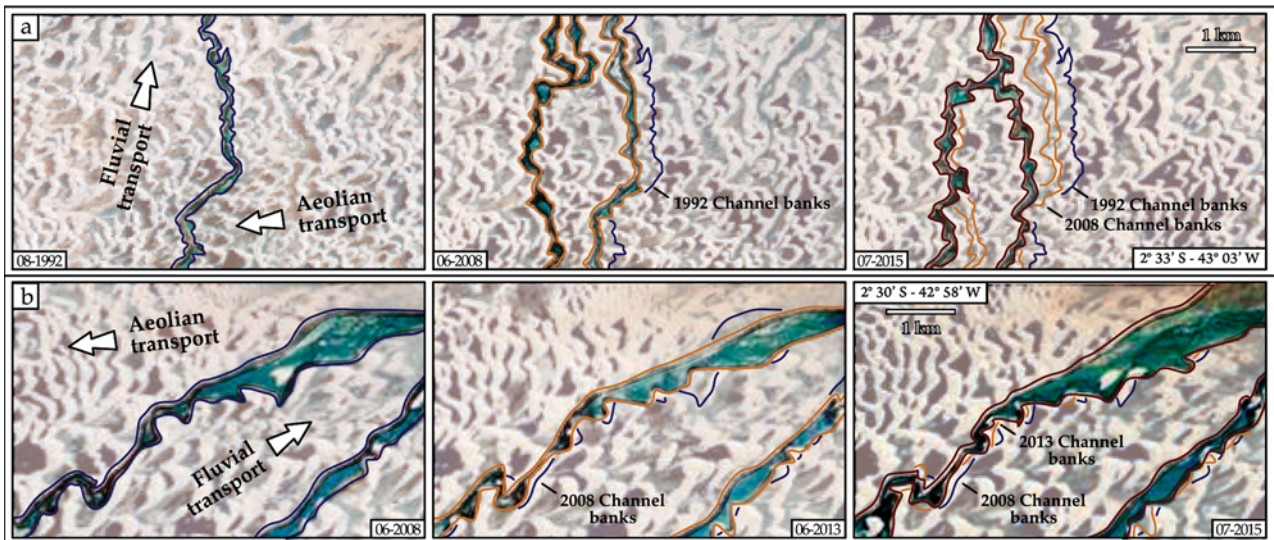


Figure 3. (Colour online) Fluvial–aeolian morphodynamics recorded at two sites along the Rio Negro, from Landsat™ false-colour remotely sensed images. The locations of fluvial channels have been highlighted. See Figure 2b for site locations. (a) Fast migration ($\sim 25 \text{ m year}^{-1}$) of trunk channels oriented parallel to aeolian-dune crests. (b) Comparatively slower ($< 10 \text{ m year}^{-1}$), oblique migration of trunk channels draining in a direction near-opposite to the direction of aeolian transport.

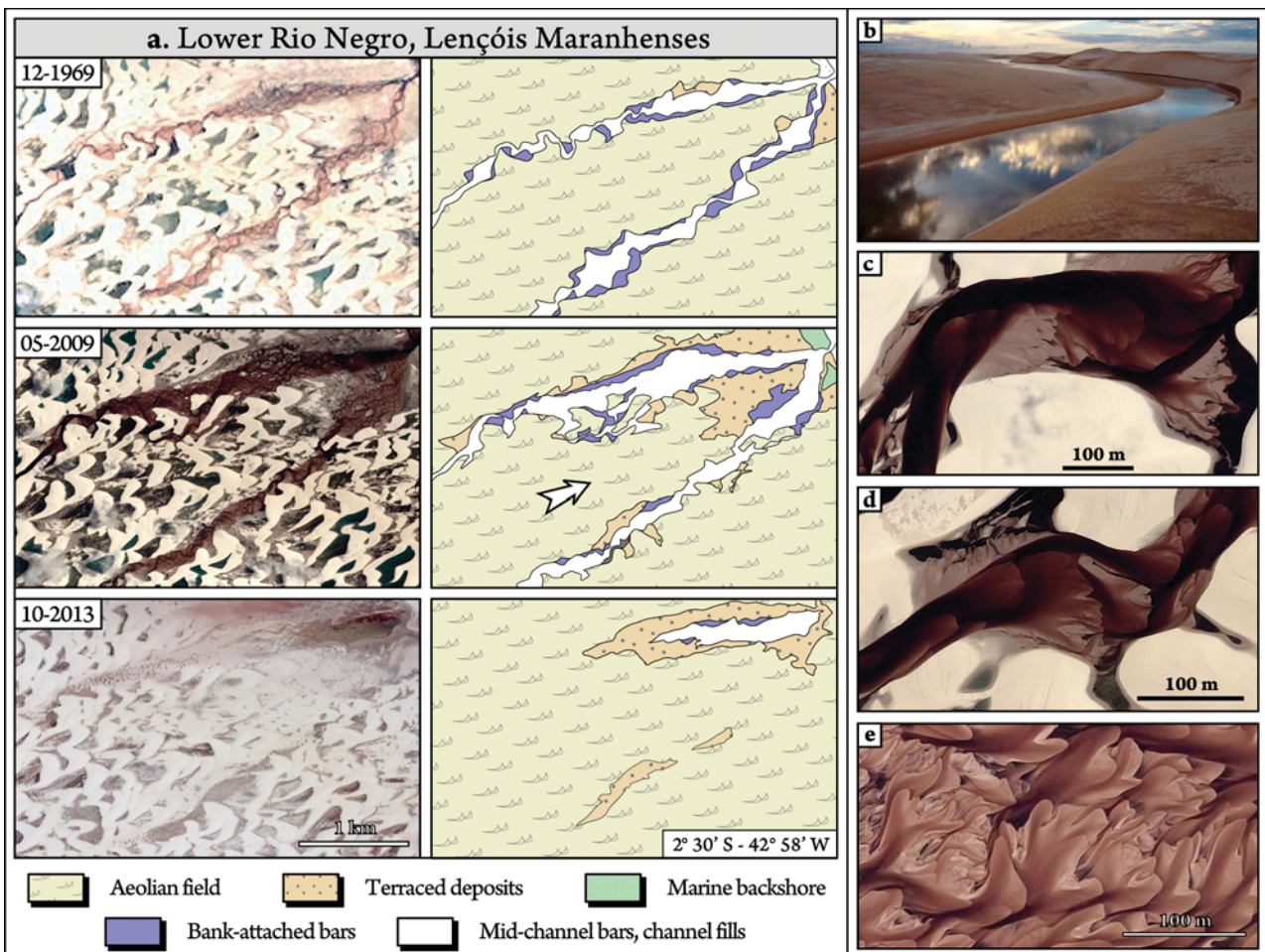


Figure 4. (Colour online) Fluvial–aeolian morphodynamics recorded in the lower Rio Negro transecting the Lençóis Maranhenses, highlighting the growth of bank-attached bars. See Figure 2b for site location. (a) Interpreted aerial photographs and high-resolution satellite scenes displaying upstream sinuous, single-threaded trunks alternating with braided-channel belts. (b) Field aspect of a channel sided by active aeolian dunes. Foreground is $c. 5 \text{ m}$ wide. Image courtesy of Simone Bessa, distributed under Creative Commons Licence CC BY-NC-SA 2.0. (c–e) Planform aspect of point bars (c), side bars (d), and compound transverse bars (e) (May 2009 scene).

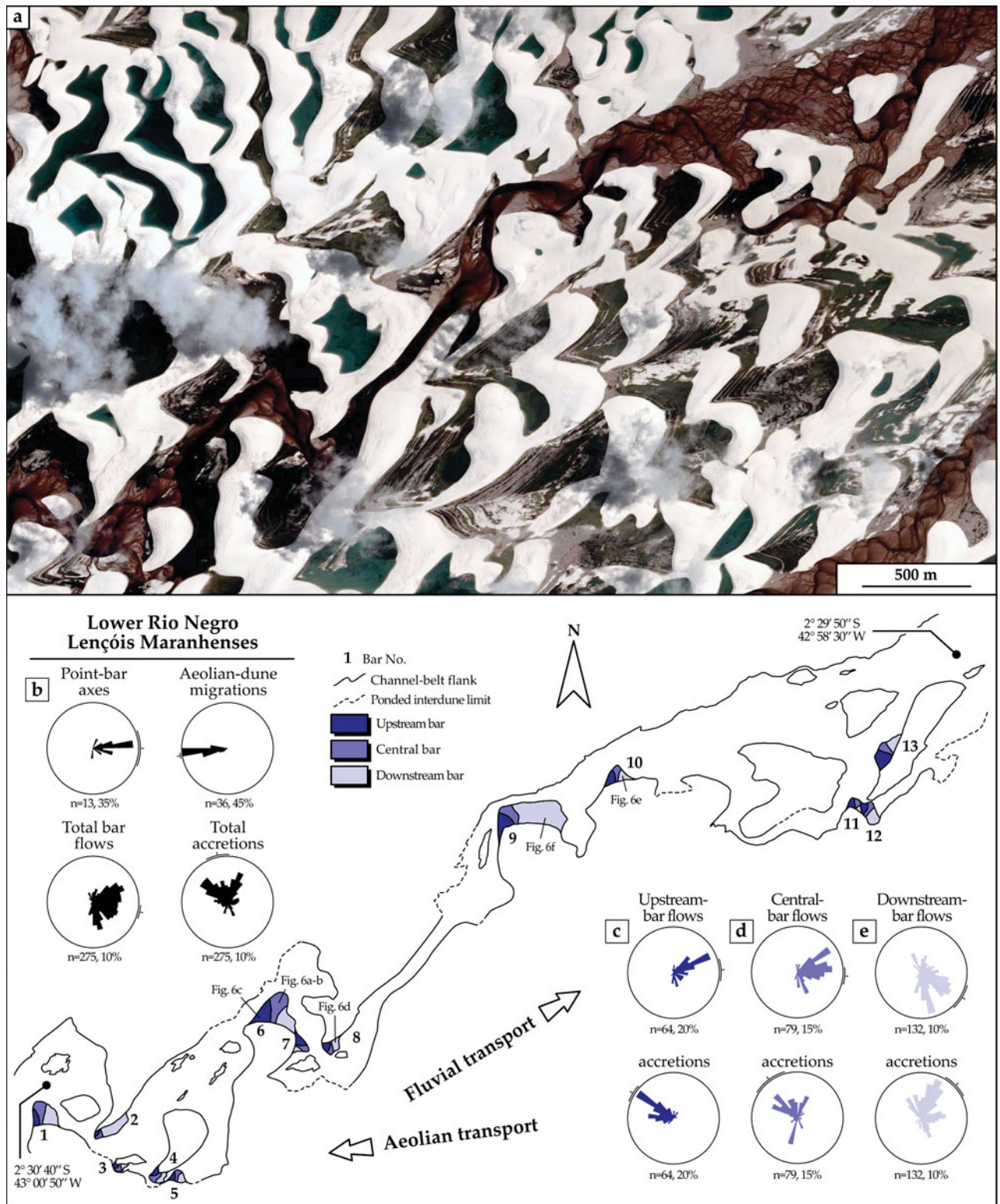


Figure 5. (Colour online) Planform aspect and sediment-transport patterns of 13 point bars occurring along a mildly sinuous, single-threaded to braided tract of the Rio Negro transecting the Lencóis Maranhenses. (a) Un-interpreted, high-resolution satellite view of the study transect. The satellite image was acquired in May 2009, see Figure 2b for location. (b–e) Rose diagrams report average vector and 95% confidence arc for total values (b), and upstream- (c), central- (d), and downstream- (e) bar portions, respectively. See Figure 6a for detailed insets and methods of data collection.

3.b. Point-bar geometry and drainage

The salient features of 13 point bars in a 5 km long clear-water transect of the satellite scene of May 2009 (Figs 4, 5) are reported in Table 1. Point bars range

in radius from 40 to 150 m (mean = 75 m), and their channel-ward outbuilding is consistent with expansional mechanisms (i.e. bar growth in a direction roughly normal to the channel axis; Allen, 1982). Bar outbuilding is mediated by the coalescence of unit bars

Table 1. Morphologic features of the unvegetated point bars of the Rio Negro, Lençóis Maranhenses. Bar numbering refers to Figure 5.

Bar No.	Hydrographic bank	Axis orientation	Point-bar radius (m)	Channel width (m)	Radius to ch. width	Chute drainage	Angle of impingement	Downstream-flow separation
1	Right	87°	115	245	0.5	No	35°	None
2	Left	76°	65	160	0.4	No	75°	Modest, with pool development
3	Left	110°	35	40	0.9	No	15°	None
4	Left	127°	45	50	0.9	No	70°	Modest, with pool development
5	Right	85°	50	60	0.8	Yes	50°	None
6	Right	103°	150	245	0.6	Yes	35°	None
7	Right	187°	65	155	0.4	No	40°	None
8	Left	63°	60	70	0.9	Yes	65°	Modest, with pool development
9	Right	87°	100	145	0.7	No	85°	Strong, with bank collapse
10	Right	75°	70	175	0.4	No	30°	None
11	Right	98°	50	170	0.3	No	40°	None
12	Right	88°	65	85	0.8	No	30°	None
13	Right	25°	85	170	0.5	Yes	80°	Strong, with bank collapse

(sensu Smith, 1977) with a transverse planform that migrate in the deeper portions of the channel (cf. Hooke, 1986). The observed point bars further show a slightly preferential downstream growth. The ratio between point-bar radius and the attached-channel width ranges from 0.3 to 0.9, averaging 0.6 (considering the width of the originating channel rather than that of the entire channel belt). A direct correlation exists between the point-bar radius and the width of the originating channel:

$$r = 0.37(w) + 23 \tag{1}$$

where *r* and *w* are the point-bar radius and parent-channel width (metres), respectively, with $R^2 = 0.65$. This correlation is to some extent parallel to the meander Cartesian length to channel width ratio typical of conventional meandering rivers (cf. Seminara, 2006). An angle of *c.* 160° exists in between the average fluvial (N 60°) and aeolian (N 260°) transport directions (Fig. 5). Point bars are preferentially preserved on hydrographic right-hand banks (9 out of 13; Fig. 5a) owing to a westward shift of the fluvial trunks (Fig. 3), and face upwind with respect to the direction of aeolian transport. In all instances, point bars transition channelward into compound transverse bars (Fig. 6a, b), 15 to 40 m wide (exceptionally up to 70 m) and as much as 110 m long. A scroll topography is not directly evident. Scroll topography is either absent or, if subdued, it is possibly masked by lacking contrast in vertical imagery. However, a gradient in decreasing current velocity when approaching the point-bar waterline brings about the local migration of unit bars in an oblique, channel-bankward direction (Fig. 6a, b). Point bars have subdued relief owing to the shallow nature of the originating channels, and are largely submerged during stages of active fluvial drainage (Fig. 3b), with unit, transverse bars free to climb up-bar over the entire span in between the channel pool and flank (Fig. 6a). Evidence of top cross-cut is present in 4 of

the 13 point bars, and consists of chute channels draining the inner point-bar portions, and feeding in some instances small frontal chute bars (sensu Ghinassi, 2011; Fig. 6c).

All the point bars have upstream, central and downstream portions (23 %, 29 % and 48 % of total surface, respectively), with central point-bar portions facing the channel pool in the area of maximum bend curvature (Ielpi & Ghinassi, 2014). In the upstream bar portions (Fig. 5c), unit transverse bars migrate downstream with directions consistent with that of the parent channel, and the standard deviation of 64 flow indicators is 60°. Bar accretion is overall oriented upstream, forming angles with the channel axis of $170^\circ \pm 90^\circ$. A similar pattern is evident in the central-bar portions (Fig. 5d), where 79 flow indicators are oriented downstream to slightly inner bankwards with a standard deviation of 52°. The respective bar accretions point to upstream to bankward directions, forming angles with the channel axis of $130^\circ \pm 120^\circ$. In the downstream portions (Fig. 5e), 132 flow indicators show bankward to upstream transport, with a standard deviation of 85°. Bar accretion points to downstream to outer-bankward growth, forming angles of $30^\circ \pm 110^\circ$ with the channel axis.

Along the downstream-most point-bar portions, different planforms occur depending on the angle of impingement of the channel flow onto the inner bank, and subsequent separation of the channel flow itself (cf. Burge & Smith, 1999). At low angles of impingement (< 50°), the flow is readily deviated in a direction near-parallel to the channel axis, and no significant flow separation takes place (Fig. 6a). At angles between 50° and 70°, partial flow separation generates eddy currents that scour deep pools (Fig. 6d). At angles of impingement higher than 70°, flow separation induces channelward migration of unit transverse bars, bank collapse (Fig. 6e), and cohesion-less deposits introduced into the channel are washed away or nucleate proto-side bars (Fig. 6f).

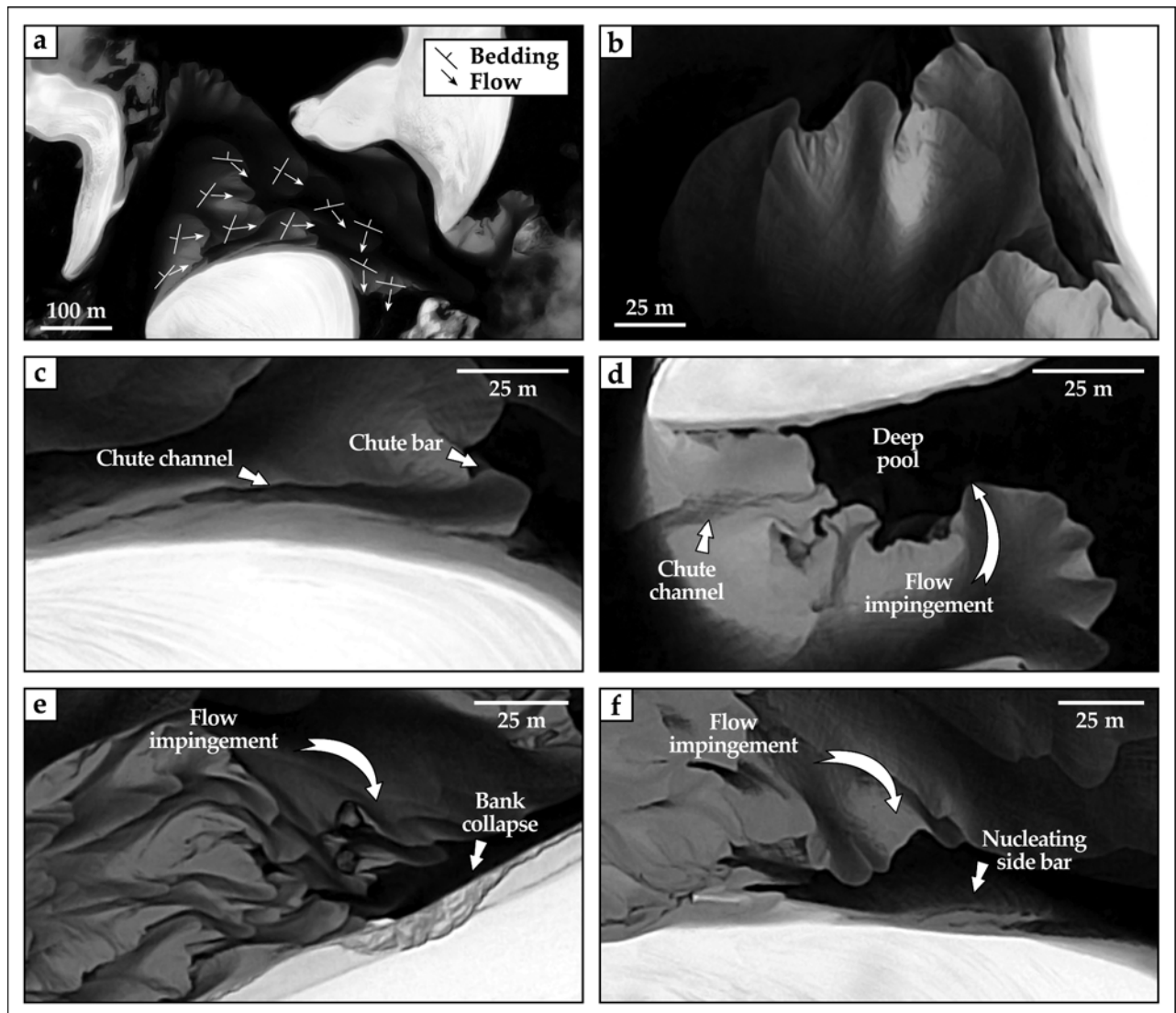


Figure 6. Panchromatic, high-resolution satellite views of modern unvegetated point bars of the lower Rio Negro transecting the Lençóis Maranhenses. See Figure 5b for inset locations. (a) Vectors of lateral-bar growth (streaked lines, with minor axis indicating accretion) and sediment transport (arrowed lines) collected along unit bars with a transverse planform and coalescing with point bars. (b) Detail of large, submerged unit (transverse) bars, coalescing with an outbuilding point bar on their hydrographic right. The unit bar shows undulate morphology, and the point bar lacks apparent scroll topography. (c) Details of active chute drainage in the submerged, bankward portion of a point bar. (d) Detail of chute drainage abutting in a relatively deep pool, the latter scoured by channel-flow separation along the bar tail. (e, f) Effects of channel-flow impingement at high angles against the inner bank, producing bankward migration of unit bars with transverse planform, bank collapse (e), and reworking of collapsed deposits into proto-side bars (f).

4. Comparison with vegetated meandering rivers

Tracts of the Beaver and Powder rivers of Alberta (Canada) and Montana (USA) are compared to the Lençóis Maranhenses, because of their similar scale and well-studied morphodynamics (Gay *et al.* 1998; Nicoll & Hickin, 2010 and references therein). The Beaver River meander belt occupies a small valley where point bars undergo downstream migration owing to spatial confinement (Fig. 7). By comparison, the Powder River meander belt lies within a larger alluvial plain, and its bends are free to expand laterally without spatial confinement (Fig. 8). Point bars are the dominant element in both rivers; mid-channel bars also occur, but tend to be incorporated into and reworked by point bars. Vegetated point bars are exposed during periods

of average channel hydrographs (Figs 7, 8), and display a well-developed scroll topography, which is controlled by the migration of bedforms and unit bars 10 to 100 times smaller than the entire point bar (Fig. 7e, f).

In a 5 km long transect of the Beaver River (Fig. 7), downstream-migrating point bars lack evidence of chute cut-off, and occupy almost entirely the narrow alluvial plain. Ratios of channel-belt width to bar radius range from 1.0 to 1.4. These values are smaller than, but comparable to, those of the studied unvegetated point bars (Table 2). Because of spatial confinement, point-bar axes are well clustered (Fig. 7a), and the meander belt displays a high degree of symmetry. The most striking difference from unvegetated point bars is the prominence of downstream migration, which induces cannibalization of upstream- and

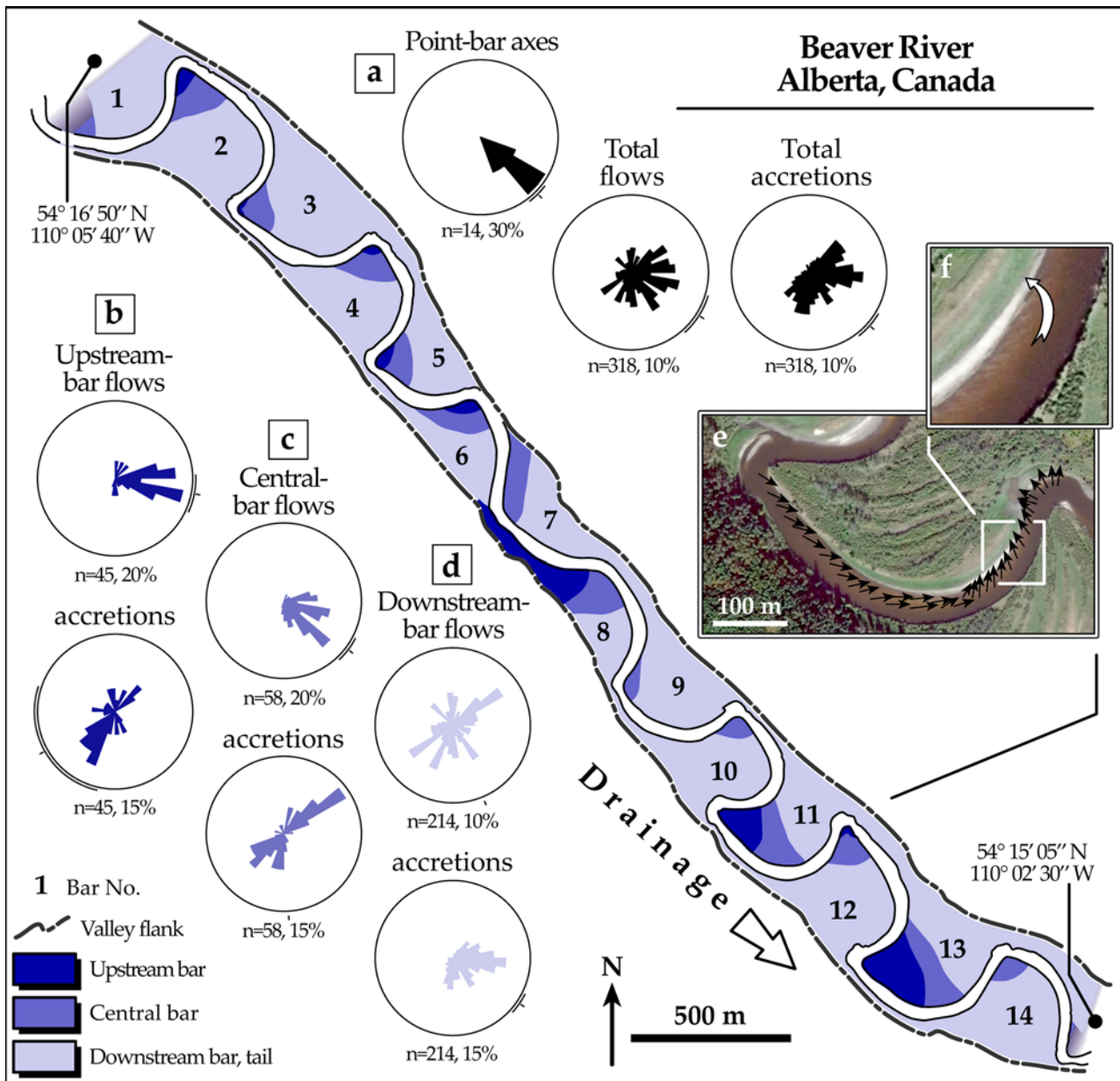


Figure 7. (Colour online) Comparative analysis of a vegetated, valley-confined meander belt (Beaver River, Alberta, Canada), featuring downstream-migrating point bars. The meander belt has high symmetry and preferential preservation of downstream-bar portions. (a–d) Rose diagrams report average vector and 95 % confidence arc for total values (a), and upstream- (b), central- (c), and downstream- (d) bar portions, respectively. Collection of accretion and flow indicators followed the criteria illustrated in Figure 6a. (e, f) Details of scroll topography generated by accretion of bedforms and small unit bars.

central-bar portions. The latter two display unimodal, downstream-oriented transport and bimodal accretion (Fig. 7b, c). On the other hand, helicoidal flows along downstream-bar portions induce high dispersion in transport, but clustered, downstream-verging accretion (Fig. 7d). Along downstream-bar bends, channel-flow impingement against the inner bank favours bank collapse and accretion of point-bar tails (Fig. 7e; cf. Smith *et al.* 2009). Angles of impingement reach 120° in places, significantly higher values than those observed in unvegetated downstream-bar portions (Table 1).

In a 3.5 km long transect of the Powder River (Fig. 8), expansional point bars occupy relatively small portions of the alluvial plain and are commonly cut by

mature chute channels. Ratios of channel-belt width to bar radius range from 3.5 to 21, values significantly higher than both unvegetated and vegetated-confined point bars (Table 2). Point bars have fairly clustered axes and a symmetric disposition (Fig. 8a). Similarly to unvegetated point bars, expansional behaviour is related to similar preservation of upstream-, central- and downstream-bar portions. However, downstream-flow impingement against the inner bank is at angles lower than 70°, and no bank collapse or bar-tail accretion occurs. Flow indicators are dispersed in the upstream- and downstream-bar portions (Fig. 8b, d), while they fan over *c.* 90° in the central-bar portions (Fig. 8c). Accretions are mildly dispersed in the upstream- and

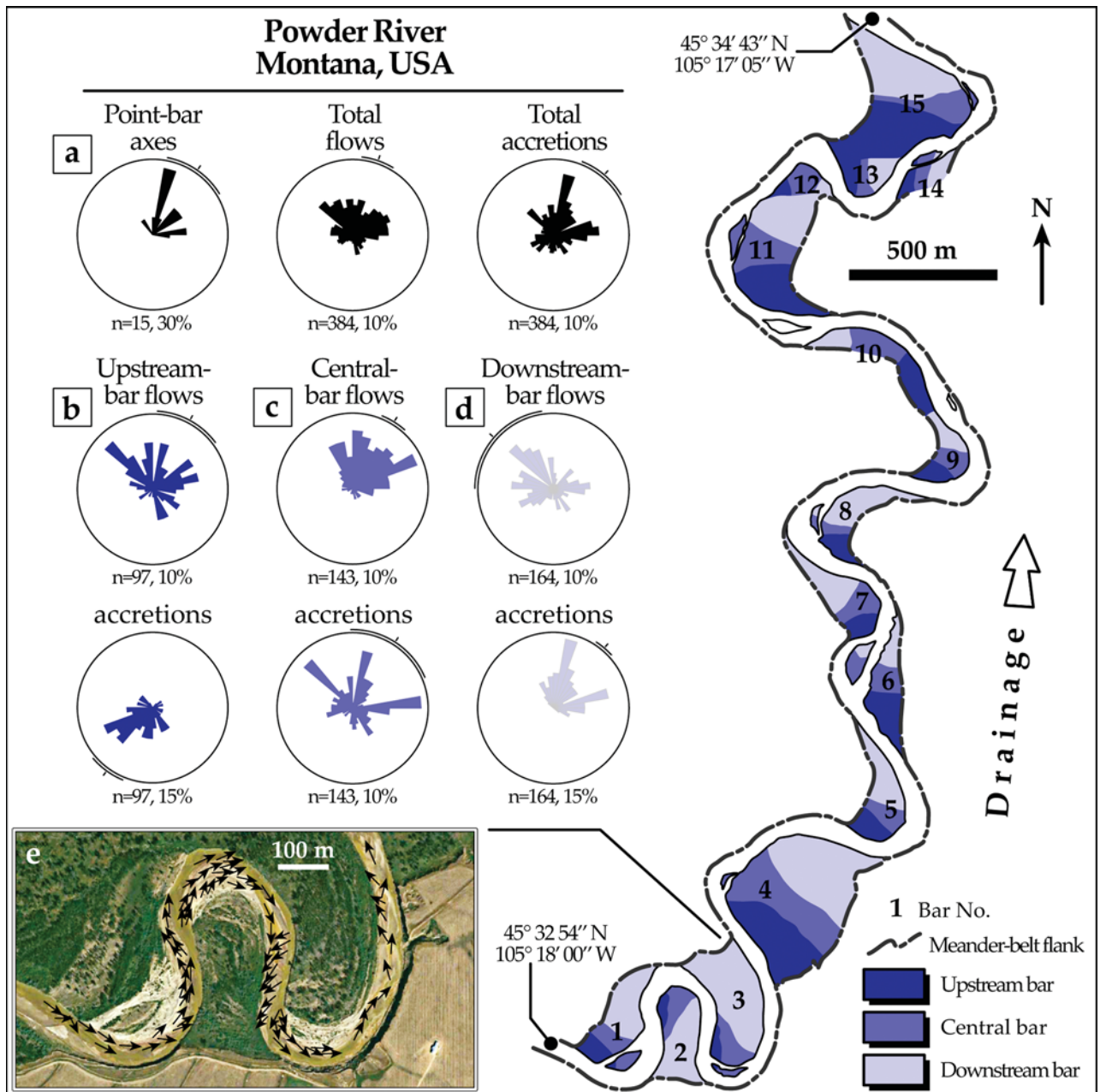


Figure 8. (Colour online) Comparative analysis of a vegetated, unconfined meander belt (Powder River, Montana, USA), featuring expansional point bars. The meander belt has high symmetry and comparable preservation of upstream-, central- and downstream-point bar portions. (a–d). Rose diagrams report average vector and 95 % confidence arc for total values (a), and upstream- (b), central- (c), and downstream- (d) bar portions, respectively. Collection of accretion and flow indicators followed the criteria illustrated in Figure 6a. (e) Detail of scroll topography, in places cross-cut by mature chute channels.

downstream-bar portions, and polymodal in the central-bar portions.

5. Discussion

5.a. Controls on fluvial-planview style

The development of meandering planforms responds to a number of factors, including self-organization (Stølum, 1996; Smith, 1998), equilibrium between runoff and sediment supply (Hooke, 2007) and, more generically, substrate roughness relative to slope gradient (Lazarus & Constantine, 2013). In fluvial–aeolian

systems such as the lower Rio Negro transecting the Lençóis Maranhenses, grain size and morphology of supplied sediment are largely influenced by aeolian processes, so that sediment tends to be homolithic and deprived of mud fractions (cf. Smith & Smith, 1984). When aeolian dunes composed of non-cohesive sediment migrate in a direction oblique to opposite to that of fluvial drainage, they provide spatial confinement to the channel belt (cf. Langford, 1989; Bullard & McTanish, 2003), thus hampering its expansion and inducing substrate roughness (Lazarus & Constantine, 2013). These processes aid the development of point bars along sharp bends, in concert with the low topographic gradient

Table 2. Comparative features of unvegetated, vegetated-confined and vegetated-unconfined point bars of Figures 5–8.

		Unvegetated	Vegetated confined	Vegetated unconfined
Point-bar behaviour		Expansional	Downstream-migrating	Expansional
Scroll topography		No	Yes	Yes
Channel-belt width : bar radius		1.1–14.5	1.0–1.4	3.5–21.0
Channel-belt symmetry		Low	High	High
Upstream-central preservation		High	Low	High
Chute drainage		Developed	Absent	Well developed
Downstream-flow separation		In places	Common	Absent
Point-bar axes		Clustered, inconsistent with trunk axis	Clustered, consistent with trunk axis	Dispersed
Upstream	Flow	Downstream, clustered	Downstream, clustered	Dispersed
	Accretion	Upstream, clustered	Clustered, bimodal	Upstream, polymodal
Central	Flow	Downstream, mildly dispersed	Downstream, clustered	Downstream, polymodal
	Accretion	Dispersed	Clustered, bimodal	Downstream, polymodal
Downstream	Flow	Dispersed	Dispersed	Dispersed
	Accretion	Downstream, mildly dispersed	Downstream, polymodal	Downstream, bimodal

typical of coastal settings. Notably, these morphodynamics are characteristic of single-thread channels, braided channels and anabranches located on their sides (Fig. 5).

The absence of floodplain tracts or local spring lines within the Lençóis Maranhenses brings about funneling of discharge into the main channel trunks, a process aided by overspill from adjacent lagoons mediated by the migration of aeolian dunes. The hydrology of the Rio Negro is also seasonally influenced by the groundwater-table height within the aeolian-dune field. Within the trunk channels, higher hydrographs are capable of mobilizing larger quantities of aeolian sand, and bedload starvation is unlikely, preventing the complete reworking and wash-over of point bars at bankfull depth (Bluck, 1974). In the upstream reaches of the study transect, an equilibrium exists between discharge and sediment supply, and conditions are favourable for point-bar growth in alternating single-thread to braided trunks. Continuous addition of sediment by aeolian-dune migration eventually generates surplus, and the downstream transition into a fully braided planform takes place (Smith & Smith, 1984).

5.b. Unvegetated v. vegetated point bars

Unvegetated point bars in fluvial–aeolian settings linearly scale with the width of their parent channel, a feature shared with tidal and vegetated fluvial meanders, the latter both confined and unconfined (Seminar, 2006). However, unvegetated point bars of the Lençóis Maranhenses show preferential growth and preservation on hydrographic right-hand banks, owing to leftward (i.e. westward) channel-belt migration (Fig. 9). Also, bank erosion is facilitated on hydrographic left-hand banks, which are located downwind of the main aeolian-transport direction. There, aeolian sand accumulates in steep dune-lee faces that abut onto unstable banks (Al-Masrahy & Mountney, 2015; Fig. 9). The preferential occurrence on one bank relates

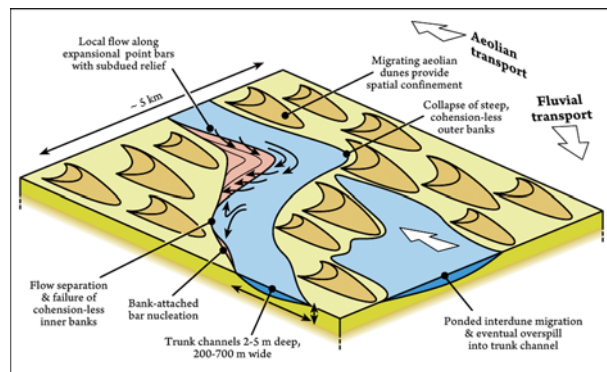


Figure 9. (Colour online) Summary of the depositional morphodynamics and fluvial–aeolian interactions observed in the sinuous fluvial tracts transecting the Lençóis Maranhenses. Scale is indicative, although the relative sizes of aeolian dunes and fluvial channels are consistent. See discussion in the text.

to lateral accretion overall perpendicular to the vector of aeolian-dune migration (Fig. 5a), rather than dispersed and overall downstream-oriented as in vegetated systems (Figs 7a, 8a). Also, preferential disposition of point bars on one bank hampers the development of bimodal or strongly divergent total directions of sediment transport and accretion (cf. Todd & Went, 1991), which are instead observed in vegetated systems (Table 2; Figs 7a, 8a). Lower flow dispersion can also be a reflection of the relatively low sinuosity of the unvegetated system, as well as of absence of interference with floodplain flows re-entering the channel after high-flood stages.

When compared to vegetated meanders, subdued bar relief exerts a strong morphodynamic control: 30 % of point bars exhibit chute drainage (Table 1), which indeed is facilitated atop low-relief point bars that are fully submerged during most of the channel belt active life. In concert with sediment supply, subdued bar relief also favours the superimposition of large unit bars reaching hundreds of metres in width and downstream extent (Fig. 6a, b). In turn, the coalescence of

unit bars with a scale comparable to that of point bars hampers the development of apparent scroll topography. The development of scroll topography is also possibly hindered by the low relief of the point bar itself, in turn an effect of bar growth within shallow, broad channels. Despite the spatial confinement induced by the surrounding topography, the channel-belt shift induced by aeolian-dune migration allows for the expansion (rather than downstream migration) of point bars located on the trailing bank. This apparent contrast between expansional morphodynamics and spatial confinement portrays an intermediate model for unvegetated point bars. In fact, the studied point bars are featured by sub-equal preservation of upstream-, central- and downstream-bar portions, yet with well-developed flow separation along their tails (Table 1; Fig. 6). These features are typically complementary in vegetated systems (Smith *et al.* 2009).

The expansional rather than downstream-migrating behaviour of spatially confined point bars can be related to their relatively small size when compared to that of the parent channel (Table 1), or to the lack of cohesive banks resistant to erosion. In the Lençóis Maranhenses, downstream-flow impingement with angles of 70° is sufficient to generate bank collapse. By comparison, in both modern and ancient meandering-fluvial deposits, similar processes require angles of impingement of up to 120° (Smith *et al.* 2009; Ielpi & Ghinassi, 2014), owing to cohesive mud-rich banks or plant stabilization. This peculiarity points to higher efficiency of flow impingement in destabilizing unvegetated banks (Fig. 9). On the other hand, lower angles of impingement hinder a flow separation prominent enough to generate eddy accretions or counter-point bars (cf. Smith *et al.* 2009). Instead, downstream-bar flows are responsible for the scouring of deep pools prone to host bank-collapse deposits (Fig. 6e). Since these processes assist in some instances the nucleation of new bank-attached bars (Fig. 6), a weak feedback loop can be envisaged (cf. Rhoads & Welford, 1991; Fig. 9).

5.c. Perspective on the Precambrian rock record

The lower Rio Negro bears evidence for the alternation of moderately sinuous single-threaded channels and braided-channel belts within the Lençóis Maranhenses (Fig. 5). High- to low-sinuosity transitions have been previously discussed for vegetated rivers (Schwartz, 1978; Schumm, 1981), but not for unvegetated counterparts. However, extra-terrestrial fluvial landscapes featuring aggradational transitions from a straight to meandering planform are documented (Bhattacharya *et al.* 2005), suggesting shared mechanisms of planform change in vegetation-free landscapes (Fig. 10a). The absence of apparent scroll topography in favour of large, coalescent unit bars may introduce significant overlap with low-sinuosity fluvial models (Cant & Walker, 1978b). Growth of point bars with subdued topography as in the Lençóis Maranhenses is likely to generate sedimentary bodies with very low-angled

accretionary surfaces, another potential source of overlap with the sedimentary products of low-sinuosity rivers (Ghinassi & Ielpi, 2015). It follows that the proper characterization of pre-vegetation point bars in the rock record may be biased unless observed in plan-view, or along 3D sections where the comparison of channel and bar palaeodrainage is possible.

The propensity of cohesion-less banks to collapse when impacted by channel flow at relatively low angles is consistent with the abundance of soft-sediment deformation structures in Precambrian fluvial units (Long, 2011). Furthermore, sinuosity in unvegetated systems could have been aided by bank strengthening associated with external factors, such as permafrost (Fairén *et al.* 2014; Fig. 10b), precipitation of metals, either microbially mediated or not (Fernández-Remolar *et al.* 2005; Fig. 10c), or microbial sediment binding (Prave, 2002). Sediment cohesion in mud-rich environments may also have aided bank strengthening (Fralick & Zaniewski, 2012), but this latter factor is hard to assess given the overall scarcity of fine-grained deposits in contexts where aeolian processes are prominent. As such, the results of this study should be applied to sand-dominated fluvial systems that largely lacked the effects of cohesive banks (cf. Ielpi & Ghinassi, 2015), while the morphodynamics of pre-vegetation mud-prone systems may have differed significantly (cf. Santos & Owen, 2016).

As the processes observed in this study have decadal scales, few inferences can be made from the study of modern fluvial–aeolian systems on their long-term preservation. Accommodation is of course pivotal and, although with scarce chronological constraint, strongly aggradational basin tracts are more likely to have preserved high-sinuosity fluvial forms, a condition somewhat favourable along Precambrian intracratonic successions (Eriksson *et al.* 1998). Independent from accommodation, long-term preservation of unvegetated point bars is likely to be the highest for large, stable forms located on accretionary banks somewhat protected by aeolian-dune migration. Fast and extensive reworking associated with outburst floods militates against sinuosity, even at the decadal scale (Bluck, 1974; Schwartz, 1978; Fig. 10d, e), hence fluvial successions bearing evidence of flashy discharge (e.g. Hjellbakk, 1997; Long, 2006) are less prone to have any point bars preserved. Though not the case in this study, absence of vegetation may also have promoted rapid hydrograph rising (Davies & Gilbing, 2010), possibly with runoff-dominated, sediment-deprived events (cf. Long, 2006). On the other hand, systems with stable discharge during part of the year, like the ones contained in the Lençóis Maranhenses, demonstrate better preservation of their high-sinuosity fluvial tracts over decades, since large channels tend to develop prominent point bars able to survive later reworking (December 1969 and May 2009 scenes in Fig. 4a), and their size makes them less easily reworked by adjacent aeolian dunes.

Putative Precambrian analogues for the Lençóis Maranhenses could be represented by fluvial–aeolian

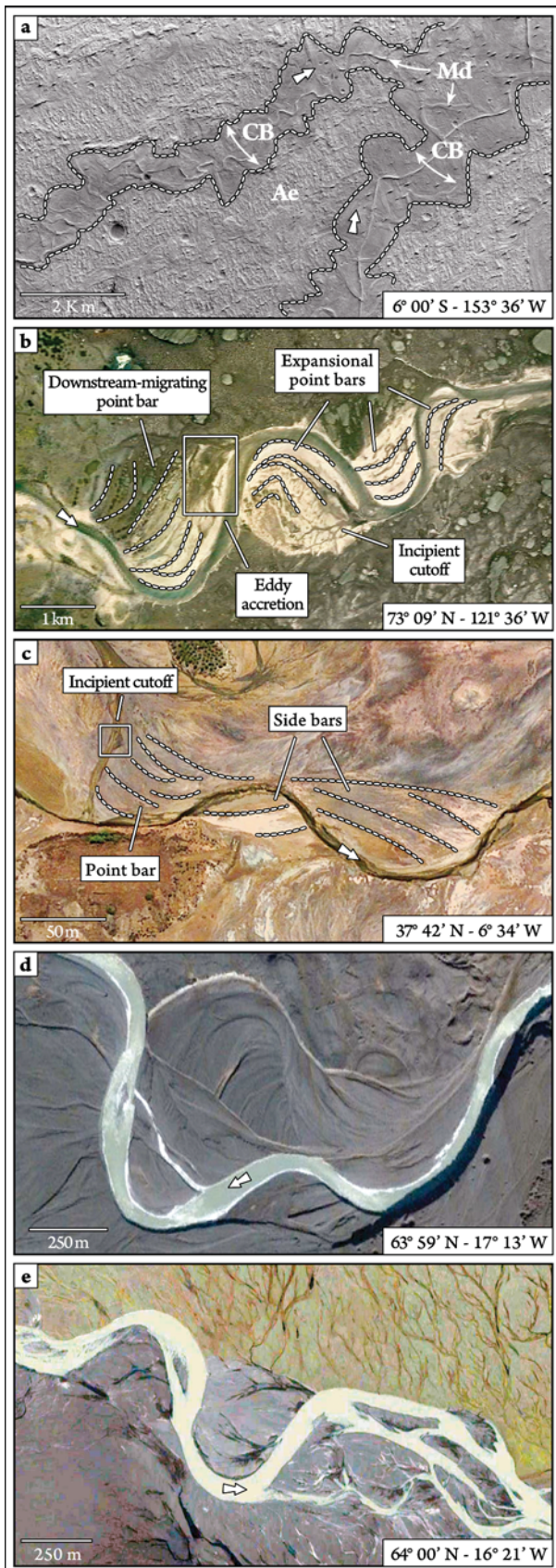


Figure 10. (Colour online) Possible external controls on the development of sinuous planforms in unvegetated to scarcely vegetated fluvial settings. Solid arrows indicate local drainage. (a) Meandering channels (Md) hosted within channel belts (CB) transecting aeolian fields (Ae) on Mars, with fluvial sinuosity possibly aided by ground ice (Fairén *et al.* 2014). (b, c) Factors

tracts contained, for example, in the 1 Ga Nelson Head Formation of the Brock Inlier and the 1.6 Ga Ellice Formation of the Elu Basin. Both these formations contain evidence of high- and low-sinuosity tracts in close association with aeolian deposits (Long, 2011; Ielpi & Rainbird, 2015, 2016). There, fluvial and aeolian deposits are observed in both planform and vertical exposures where bar and channel palaeoflow can be compared. In some instances, large-scale aeolian cross-beds (set thickness > 30 m) are scoured by channel forms hosting bank-attached bars composed of metre-scale cross-beds. These features are interpreted as typical of stable fluvial drainage between high-relief sand dunes (Ielpi & Rainbird, 2015). In this context, future directions of research should focus on, or reappraise, humid fluvial–aeolian systems like those described by Pulvertaft (1985) and Tirsgaard & Øxnevad (1998), or basin tracts where aeolian and fluvial facies are closely interbedded (cf. Hadlari, Rainbird & Donaldson, 2006).

6. Conclusions

Point bars occurring in sinuous and braided fluvial reaches of the Rio Negro, a fluvial trunk transecting the aeolian Lençóis Maranhenses of Brazil, indicate that modern unvegetated streams are not solely characterized by a low-sinuosity planform and downstream-bar accretion. Multi-temporal analysis over a timespan of *c.* 45 years shows that the rhythmic expansion of fluvial drainage is controlled by interdune connectivity, groundwater-table fluctuation and aeolian-induced spatial confinement. Growth of point bars along sharp channel bends is facilitated by low coastal topography and equilibrium between discharge and sediment supply. Continuing bedload addition from aeolian processes favours the downstream transition into wider braided-channel belts.

During periods of channel-belt activity, expansional point bars with subdued relief show accretion and migration of large superimposed unit bars that hinder the development of scroll topography. Point bars have preferential disposition on accretionary banks facing obliquely upwind into the aeolian-transport direction, a feature that strongly controls their patterns of growth and sediment transport. Unvegetated point bars display an intermediate behaviour portrayed by processes that tend to be complementary in vegetated point bars. Unvegetated point bars display expansional morphodynamics despite their spatial confinement, and are

aiding in the development of meandering-fluvial morphodynamics (e.g. point-bar growth, migration and cut-off) include permafrost (b, meander belt of Bernard River, Banks Island, Arctic Canada) and bank cementation by metal oxides (c, side and point bars of Río Tinto Basin, Spain). (d, e) Short-lived, highly sinuous planforms developed during low-stage reworking, Skeiðarár and Fjalsjökull sandurs of southeastern Iceland. Long-term preservation is there hampered by high-hydrograph floods (cf. Bluck, 1974).

featured by equal preservation of upstream, central and downstream portions, the latter with some degree of flow separation along the bar tail. There, channel-flow impingement against banks at angles higher than 70° generates deep scoured pools, bank collapse and reworking of collapsed deposits into new bank-attached bars.

Modern fluvial–aeolian landscapes such as the Lençóis Maranhenses demonstrate vast potential for the study of the morphodynamics of ancient vegetation-free depositional environments. Lack of apparent scroll topography and low bar relief introduce overlap with low-sinuosity fluvial facies models, underscoring the critical observation of ancient deposits in planform or along 3D sections where bar- and channel palaeoflow can be fully compared. While ground ice or microbial sediment binding may have provided additional bank stabilization and enhanced sinuosity in Precambrian fluvial systems, this study demonstrates that growth and preservation of point bars is also plausible in cohesion-less deposits. Preservation of fluvial point bars in the Precambrian was possibly higher in high-accommodation settings with stable fluvial discharge and low topographic gradient. On the other hand, ancient fluvial successions bearing evidence of flashy discharge and high topographic gradient are likely to be devoid of any sinuous tracts.

Acknowledgements. The ideas in this work matured during a visiting period at Dalhousie University, under the supervision of Martin Gibling. Contributions from Massimiliano Ghinassi (University of Padua) and Robert Rainbird (Geological Survey of Canada) are also acknowledged. The work benefited from insightful reviews by Philip Fralick (Lakehead University) and David Went (Oyster Petroleum). Research was supported by a research fellowship granted by the Natural Sciences and Engineering Research Council of Canada.

References

- AL-MASRAHY, M. A. & MOUNTNEY, N. P. 2015. A classification scheme for fluvial–aeolian system interaction in desert-margin settings. *Aeolian Research* **17**, 67–88.
- ALLEN, J. R. L. 1982. *Sedimentary Structures: Their Character and Physical Basis*. Developments in Sedimentology vol. 30. Amsterdam: Elsevier, 593 pp.
- ANDREWS, E. D. 1984. Bed material entrainment and the hydraulic geometry of gravel-bed rivers in Colorado. *Geological Society of America Bulletin* **95**, 371–8.
- BARTHOLDY, J. & BILLI, P. 2002. Morphodynamics of a pseudomeandering gravel bar reach. *Geomorphology* **42**, 293–310.
- BHATTACHARYA, J. P., PAYENBERG, T. H. D., LANG, S. C. & BOURKE, M. 2005. Dynamic river channels suggest a long-lived Noachian crater lake on Mars. *Geophysical Research Letters* **32**, L10201.
- BLUCK, B. J. 1974. Structure and directional properties of some valley sandur deposits in southern Iceland. *Sedimentology* **21**, 533–54.
- BRIDGE, J. S. 1993. Description and interpretation of fluvial deposits: a critical perspective. *Sedimentology* **40**, 801–10.
- BUCK, S. G. 1983. The Saaiplaas Quartzite Member: a braided system of gold- and uranium-bearing channel placers within the Proterozoic Witwatersrand Supergroup of South Africa. In *Modern and Ancient Fluvial Systems* (eds J. D. Collinson & J. Lewin), pp. 549–62. International Association of Sedimentologists, Special Publication 6.
- BULLARD, J. E. & MCTANISH, G. H. 2003. Aeolian–fluvial interactions in dryland environments: examples, concepts and Australia case study. *Progress in Physical Geography* **27**, 471–501.
- BURGE, L. M. & SMITH, D. G. 1999. Confined meandering river eddy accretions: sedimentology, channel geometry and depositional processes. In *Fluvial Sedimentology VI* (eds N. D. Smith & J. Rogers), pp. 113–30. International Association of Sedimentologists, Special Publication 28.
- CANT, D. J. & WALKER, R. G. 1978a. Fluvial processes and facies sequences in the sandy braided South Saskatchewan River, Canada. *Sedimentology* **25**, 625–48.
- CANT, D. J. & WALKER, R. G. 1978b. Development of a braided-fluvial facies model for the Devonian Battery Point Sandstone, Québec. *Canadian Journal of Earth Sciences* **13**, 102–19.
- CASTRO, A. C. L. & PIORSKI, N. M. 2002. *Plano de Manejo do Parque Nacional dos Lençóis Maranhenses, Contexto Regional*. Instituto Chico Mendes de Conservação da Biodiversidade, 40 pp.
- CHURCH, M. 2002. Geomorphic thresholds in riverine landscapes. *Freshwater Biology* **47**, 541–57.
- COTTER, E. 1978. The evolution of fluvial style, with special reference to the central Appalachians Paleozoic. In *Fluvial Sedimentology* (ed. A. D. Miall), pp. 361–84. Canadian Society of Petroleum Geologists, Memoir 5.
- DAVIES, N. S. & GIBLING, M. R. 2010. Cambrian to Devonian evolution of alluvial systems: the sedimentological impact of the earliest land plants. *Earth-Science Reviews* **98**, 171–200.
- EATON, B. C. & GILES, T. R. 2009. Assessing the effect of vegetation-related bank strength on channel morphology and stability in gravel-bed streams using numerical models. *Earth Surface Processes and Landforms* **34**, 712–24.
- ERIKSSON, P. G., BUMBY, A. J., BRÜMER, J. J. & VAN DER NEUT, M. 2006. Precambrian fluvial deposits: enigmatic palaeohydrological data from the c. 2–1.9 Ga Waterberg Group, South Africa. *Sedimentary Geology* **190**, 25–46.
- ERIKSSON, P. G., CONDIE, K. C., TIRSGAARD, H., MUELLER, W. U., ALTERMANN, W., MIALL, A. D., ASPLER, L. B., CATUNEANU, O. & CHIARENZELLI, J. R. 1998. Precambrian clastic sedimentation systems. *Sedimentary Geology* **120**, 5–53.
- ETHRIDGE, F. G., TYLER, N. & BURNS, L. K. 1984. Sedimentology of a Precambrian quartz pebble conglomerate, southwest Colorado. In *Sedimentology of Gravels and Conglomerate* (eds E. H. Koster & R. J. Steel), pp. 165–74. Canadian Society of Petroleum Geologists, Memoir 10.
- FAIRÉN, A. G., STOKES, C., DAVIES, N. S., SCHULZEMAKUCH, D., RODRÍGUEZ, J. A. P., DAVILA, A. F., UCEDA, E. R., DOHM, J. M., BAKER, V. R., CLIFFORD, S. M., MCKAY, C. P. & SQUYRES, S. W. 2014. A cold hydrological system in Gale Crater, Mars. *Planetary and Space Science* **93–94**, 101–18.
- FERNÁNDEZ-REMOLAR, D. C., MORRIS, R. V., GRUENER, J. E., AMILS, R. & KNOLL, A. H. 2005. The Río Tinto Basin, Spain: mineralogy, sedimentary geobiology, and implications for interpretation of outcrop rocks at

- Meridiani Planum, Mars. *Earth and Planetary Science Letters* **240**, 149–67.
- FRALICK, & ZANIEWSKI, K. 2012. Sedimentology of a wet, pre-vegetation floodplain assemblage. *Sedimentology* **59**, 1030–49.
- FULLER, A. O. 1985. A contribution to the conceptual modeling of pre-Devonian fluvial systems. *Transactions of the Geological Society of South Africa* **88**, 189–94.
- GAY, G. R., GAY, H. H., GAY, W. H., MARTINSON, H. A., MEADE, R. H. & MOODY, J. A. 1998. Evolution of cutoffs across meander necks in Powder River, Montana, USA. *Earth Surface Processes and Landforms* **23**, 651–62.
- GHINASSI, M. 2011. Chute channels in the Holocene high-sinuosity river deposits of the Firenze Plain, Tuscany, Italy. *Sedimentology* **58**, 618–42.
- GHINASSI, M. & IELPI, A. 2015. Stratal architecture and morphodynamics of downstream-migrating fluvial point bars (Jurassic Scalby Formation, UK). *Journal of Sedimentary Research* **85**, 1123–37.
- GIBLING, M. R. 2006. Width and thickness of fluvial channel bodies and valley fills in the geological record: a literature compilation and classification. *Journal of Sedimentary Research* **76**, 731–70.
- GRAN, K. & PAOLA, C. 2001. Riparian vegetation controls on braided stream dynamics. *Water Resources Research* **37**, 3275–83.
- HADLARI, T., RAINBIRD, R. H. & DONALDSON, J. A. 2006. Alluvial, eolian and lacustrine sedimentology of a Paleoproterozoic half-graben, Baker Lake Basin, Nunavut, Canada. *Sedimentary Geology* **190**, 47–70.
- HILBERT, N. N., GUEDES, C. C. F. & GIANNINI, P. C. F. 2016. Morphologic and sedimentologic patterns of active aeolian dune-fields on the east coast of Maranhão, northeast Brazil. *Earth Surface Processes and Landforms* **41**, 87–97.
- HJELLBAKK, A. 1997. Facies and fluvial architecture of a high-energy braided river: the upper Proterozoic Segloden Member, Varanger Peninsula, northern Norway. *Sedimentary Geology* **114**, 131–61.
- HOOKE, J. M. 1986. The significance of mid-channel bars in an active meandering river. *Sedimentology* **33**, 839–50.
- HOOKE, J. M. 2007. Complexity, self-organization and variation in behaviour in meandering rivers. *Geomorphology* **91**, 236–58.
- IELPI, A. & GHINASSI, M. 2014. Planform architecture, stratigraphic signature and morphodynamics of an exhumed Jurassic meander plain (Scalby Formation, Yorkshire, UK). *Sedimentology* **61**, 1923–60.
- IELPI, A. & GHINASSI, M. 2015. Planview style and palaeodrainage of Torridonian channel belts: Applecross Formation, Stoer Peninsula, Scotland. *Sedimentary Geology* **325**, 1–16.
- IELPI, A. & RAINBIRD, R. H. 2015. Architecture and morphodynamics of a 1.6 Ga fluvial sandstone: Ellice Formation of Elu Basin, Arctic Canada. *Sedimentology* **62**, 1950–77.
- IELPI, A. & RAINBIRD, R. H. 2016. Highly variable Precambrian fluvial style recorded in the Nelson Head Formation of Brock Inlier (Northwest Territories, Canada). *Journal of Sedimentary Research* **86**, 199–216.
- JACKSON, R. G., II. 1976. Depositional model of point bars in the lower Wabash River. *Journal of Sedimentary Petrology* **46**, 579–94.
- JEFFERSON, C. W., THOMAS, D. J., GANDHI, S. S., RAMAEKERS, P., DELANEY, G., BRISBIN, D., CUTTS, C., PORTELLA, P. & OLSON, R. A. 2007. Unconformity-associated uranium deposits of the Athabasca Basin, Saskatchewan and Alberta. In *EXTECH IV: Geology and Uranium EXploration TECHnology of the Proterozoic Athabasca Basin, Saskatchewan and Alberta* (eds C. W. Jefferson & G. D. Delaney), pp. 23–67. Geological Survey of Canada, Bulletin 588.
- LANGFORD, R. P. 1989. Fluvial-aeolian interactions: part I, modern systems. *Sedimentology* **36**, 1023–35.
- LAZARUS, E. D. & CONSTANTINE, J. D. 2013. Generic theory for channel sinuosity. *Proceedings of the National Academy of Science* **110**, 8447–52.
- LEVIN, N., TSOAR, H., MAIA, L. P., SALES, V. C. & HERRMANN, H. 2006. Dune whitening and inter-dune freshwater ponds in NE Brazil. *Catena* **70**, 1–15.
- LIU, B. & COULTHARD, T. J. 2015. Mapping the interactions between rivers and sand dunes: implications for fluvial and aeolian geomorphology. *Geomorphology* **231**, 246–57.
- LONG, D. F. G. 2006. Architecture of pre-vegetation sandy-braided perennial and ephemeral river deposits the Paleoproterozoic Athabasca Group, northern Saskatchewan, Canada as indicators of Precambrian fluvial style. *Sedimentary Geology* **190**, 71–95.
- LONG, D. F. G. 2011. Architecture and depositional style of fluvial systems before land plants: a comparison of Precambrian, early Paleozoic and modern river deposits. In *From River to Rock Record: The Preservation of Fluvial Sediments and their Subsequent Interpretation* (eds S. Davidson, S. Leleu & C. P. North), pp. 37–61. SEPM Special Publication 97.
- LUNA, M. C. DE, M., PARTELI, E. J. R., DURÁN, O. & HERRMANN, H. J. 2011. Model for the genesis of coastal dune fields with vegetation. *Geomorphology* **129**, 215–24.
- MIRANDA, J. P., COSTA, J. C. L. & ROCHA, C. F. D. 2012. Reptiles from Lençóis Maranhenses National Park, Maranhão, northeastern Brazil. *ZooKeys* **246**, 51–68.
- NICOLL, T. J. & HICKIN, E. J. 2010. Planform geometry and channel migration of confined meandering rivers on the Canadian prairies. *Geomorphology* **116**, 37–47.
- PRAVE, A. R. 2002. Life on land in the Proterozoic: evidence from the Torridonian rocks of northwest Scotland. *Geology* **30**, 811–4.
- PULVERTAFT, T. C. R. 1985. Aeolian dune and wet interdune sedimentation in the middle Proterozoic Dala Sandstone, Sweden. *Sedimentary Geology* **44**, 93–111.
- RAINBIRD, R. H. 1992. Anatomy of a large-scale braid-plain quartzarenite from the Neoproterozoic Shaler Group, Victoria Island, Northwest Territories, Canada. *Canadian Journal of Earth Sciences* **29**, 2537–50.
- RHOADS, B. L. & WELFORD, M. R. 1991. Initiation of river meandering. *Progress in Physical Geography* **15**, 127–56.
- RUST, B. R. 1981. Sedimentation in an arid-zone anastomosing fluvial system: Cooper's Creek, Central Australia. *Journal of Sedimentary Petrology* **51**, 745–55.
- SANTOS, M. G. M., ALMEIDA, R. P., GODINHO, L. P. S., MARCONATO, A. & MOUNTNEY, N. P. 2014. Distinct styles of fluvial deposition in a Cambrian rift basin. *Sedimentology* **61**, 881–914.
- SANTOS, M. G. M. & OWEN, G. 2016. Heterolithic meandering-channel deposits from the Neoproterozoic of NW Scotland: implications for palaeogeographic reconstructions of Precambrian sedimentary environments. *Precambrian Research* **272**, 226–43.
- SCHUMM, S. A. 1981. Evolution and response to the fluvial system, sedimentologic implications. In *Recent and Ancient Nonmarine Environments: Models for Exploration* (eds F. G. Ethridge & R. M. Flores), pp. 19–29. SEPM Special Publication 31.

- SCHWARTZ, D. E. 1978. Hydrology and current orientation analysis of a braided-to-meandering transition: the Red River in Oklahoma and Texas, U.S.A. In *Fluvial Sedimentology* (ed. A. D. Miall), pp. 313–42. Canadian Society of Petroleum Geologists, Memoir 5.
- SEMINARA, G. 2006. Meanders. *Journal of Fluid Mechanics* **554**, 271–97.
- SMITH, N. D. 1977. Some comments on terminology for bars in shallow rivers. In *Fluvial Sedimentology* (ed. A. D. Miall), pp. 85–88. Canadian Society of Petroleum Geologists, Memoir 5.
- SMITH, C. E. 1998. Modeling high sinuosity meanders in a small flume. *Geomorphology* **25**, 19–30.
- SMITH, D. G., HUBBARD, S. M., LECKIE, D. & FUSTIC, M. 2009. Counter point bar deposits: lithofacies and reservoir significance in the meandering modern Peace River and ancient McMurray Formation, Alberta, Canada. *Sedimentology* **56**, 1655–69.
- SMITH, N. D. & SMITH, D. G. 1984. William River: an outstanding example of channel widening and braiding caused by bed-load addiction. *Geology* **12**, 78–82.
- STØLUM, H.-H. 1996. River meandering as a self-organization process. *Science* **271**, 1710–3.
- TAL, M. & PAOLA, C. 2007. Dynamic single-thread channels maintained by the interaction of flow and vegetation. *Geology* **35**, 347–50.
- THOMAS, R. G., WILLIAMS, B. P. J., MORRISSEY, L. B., BARCLAY, W. J. & ALLEN, K. C. 2006. Enigma variations: the stratigraphy, provenance, palaeoseismicity and depositional history of the Lower Old Red Sandstone Cosheston Group, south Pembrokeshire, Wales. *Geological Journal* **41**, 481–536.
- TIRSGAARD, H. & ØXNEVAD, I. E. I. 1998. Preservation of pre-vegetational mixed fluvio-aeolian deposits in a humid climatic setting: an example from the Middle Proterozoic Eriksfjord Formation, Southwest Greenland. *Sedimentary Geology* **120**, 295–317.
- TODD, S. P. & WENT, D. J. 1991. Lateral migration of sand-bed rivers: examples from the Devonian Glashabeg Formation, SW Ireland and the Cambrian Alderney Sandstone Formation, Channel Islands. *Sedimentology* **38**, 997–1020.
- TUBINO, M., REPETTO, R. & ZOLEZZI, G. 1999. Free bars in rivers. *Journal of Hydraulic Research* **37**, 759–75.
- WILLIAMS, M. 2015. Interactions between fluvial and eolian geomorphic systems and processes: examples from the Sahara and Australia. *Catena* **134**, 4–13.
- WOOD, L. J. 2006. Quantitative geomorphology of the Mars Eberswalde delta. *Geological Society of America Bulletin* **118**, 557–66.
- ZIMMERMAN, R. C., GOODLETT, J. C. & COMER, G. H. 1967. The influence of vegetation on channel form of small streams. *International Association of Hydrological Sciences, Publication* **75**, 255–75.